Supplemental Material List

In this file

As a separate file

Table S1: Mutation dataset - this table is provided as a separate .csv text file.

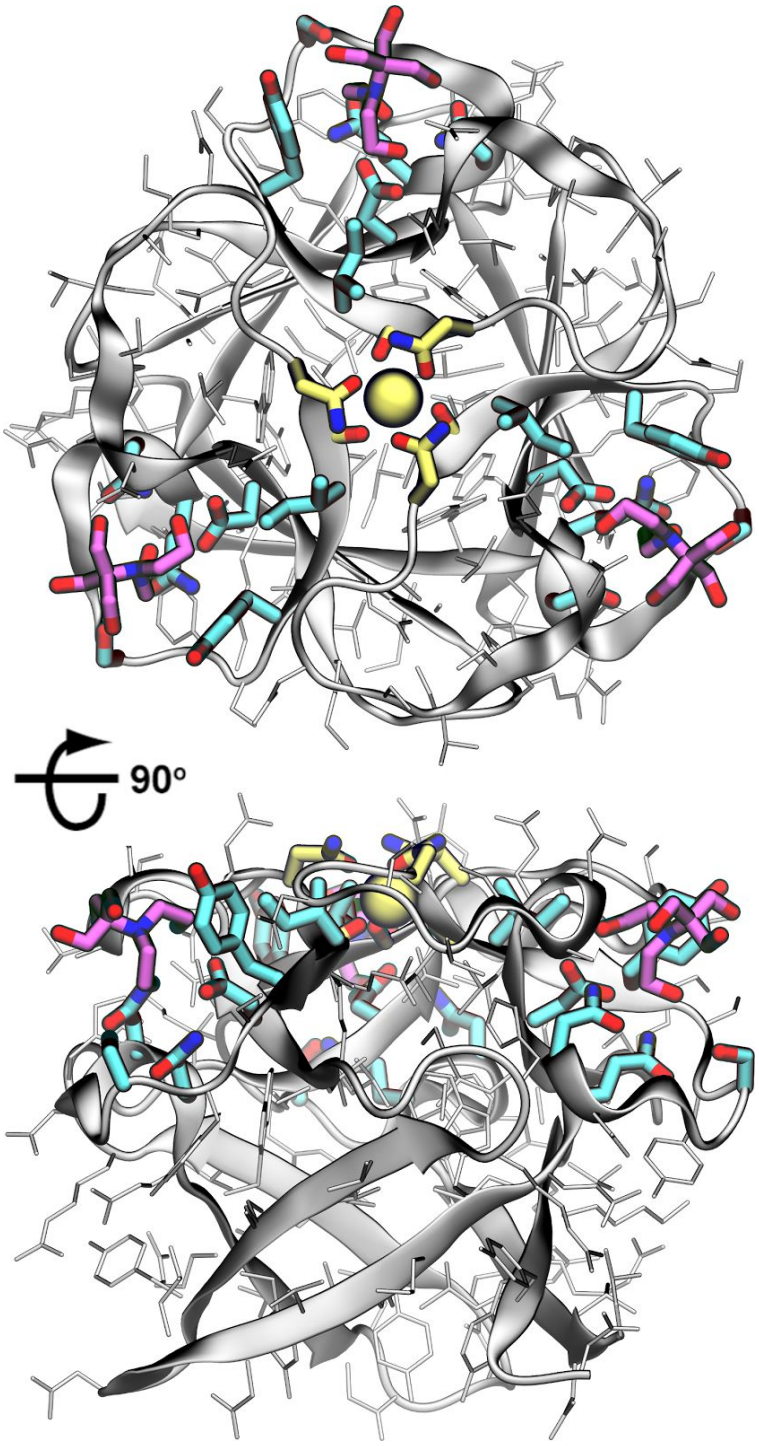

Figure S1: Functional positions excluded from mutation. Residues expected to bind carbohydrate (cyan) or sodium (yellow) binding are shown as sticks. The sodium ligand is shown as a yellow sphere and the carbohydrate mimetic ligand, bis-tris, is shown as magenta sticks. For sodium binding, the coordinating residues from the first/second/third symmetric subdomains are: asparagine (N28/N75/N122) and the backbone of valine (V29/76/123). In the case of bis-tris binding in the known carbohydrate binding site (56), the coordinating residues from the first/second/third symmetric subdomains are: D17/64/111, I30/77/124, Y32/79/126, S35/82/129, N39/86/133, and Q40/87/134. Shown using PDB: 3PG0.

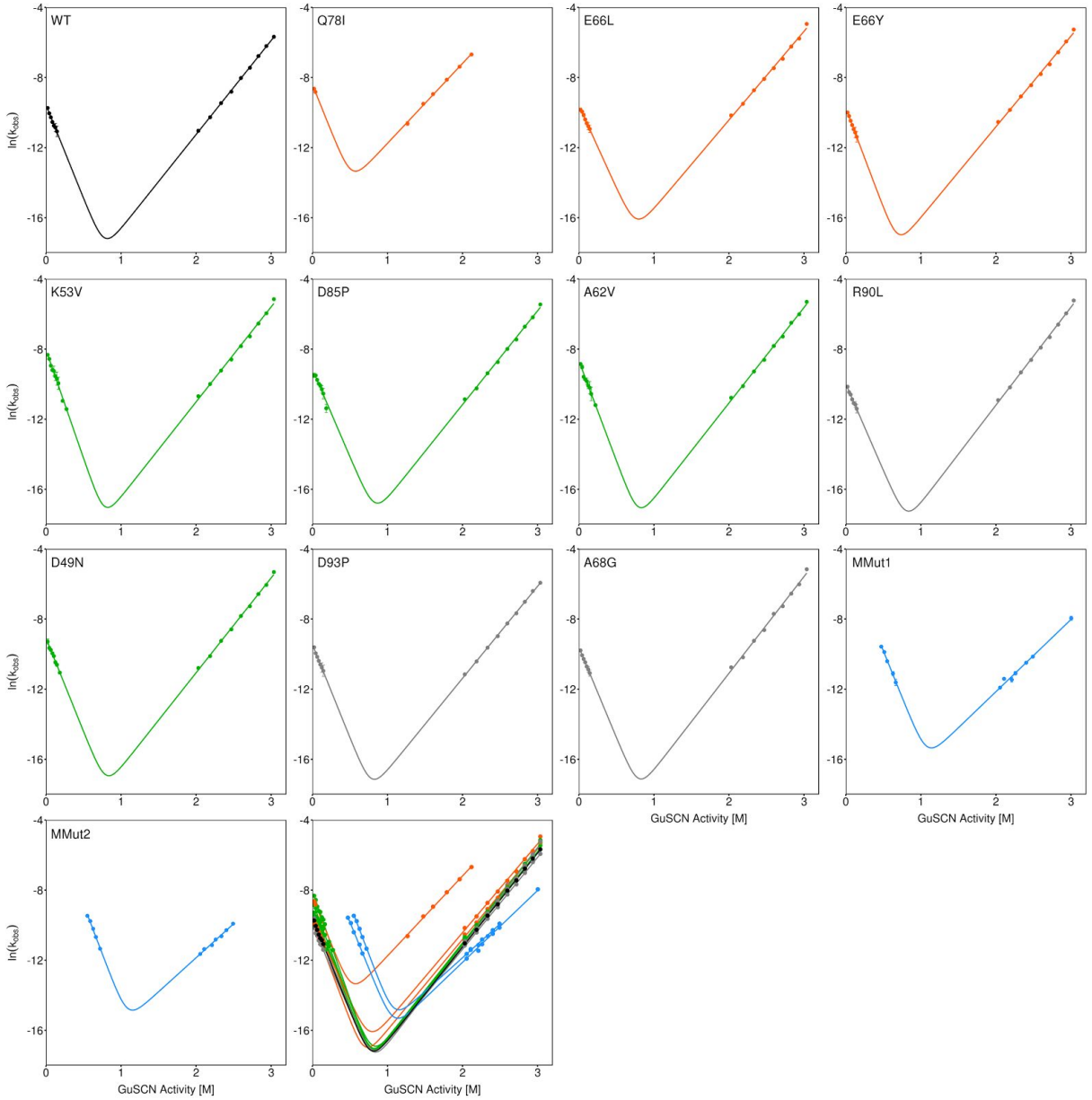

Figure S2: Kinetics of individual ThreeFoil mutants. Chevron plot of wild-type and mutant ThreeFoil kinetics. Coloring as in Figure 3b. Extrapolation of the folding and unfolding branches to 0 M denaturant is used to estimate folding and unfolding rates in water and thus thermodynamic stability (given in Table 2, also see Experimental Procedures).

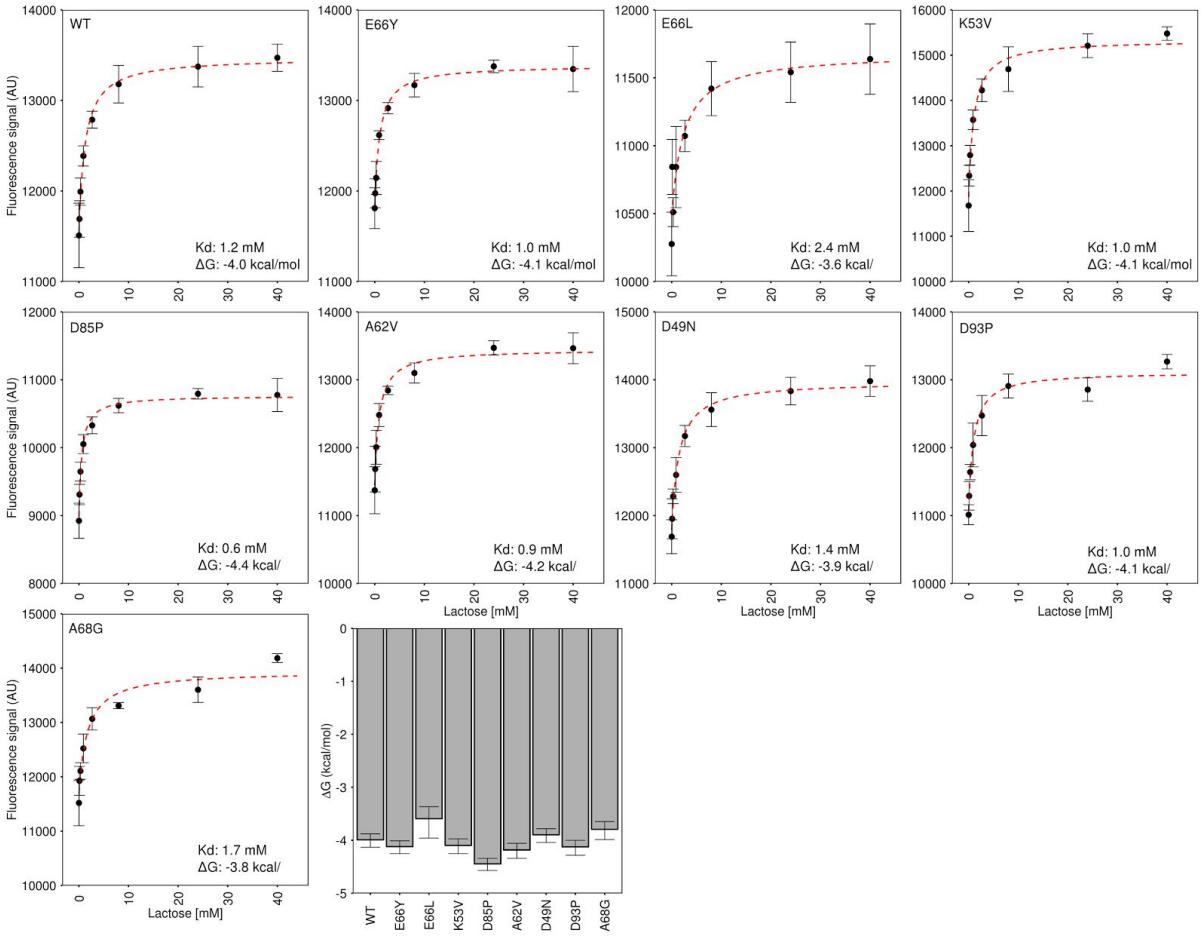

Figure S3: Stabilizing mutations do not affect sugar binding. Binding of lactose as measured by change in intrinsic fluorescence, shown for WT and selected mutants. The bottom right-hand panel shows a comparison of the $\Delta G_{binding}$ values (more -ve, stronger binding) for lactose. There is negligible change in binding across the mutants. Note that the highly destabilizing mutation Q78I, as well as the highly stabilizing multi-mutants were not tested owing to poor solubility.

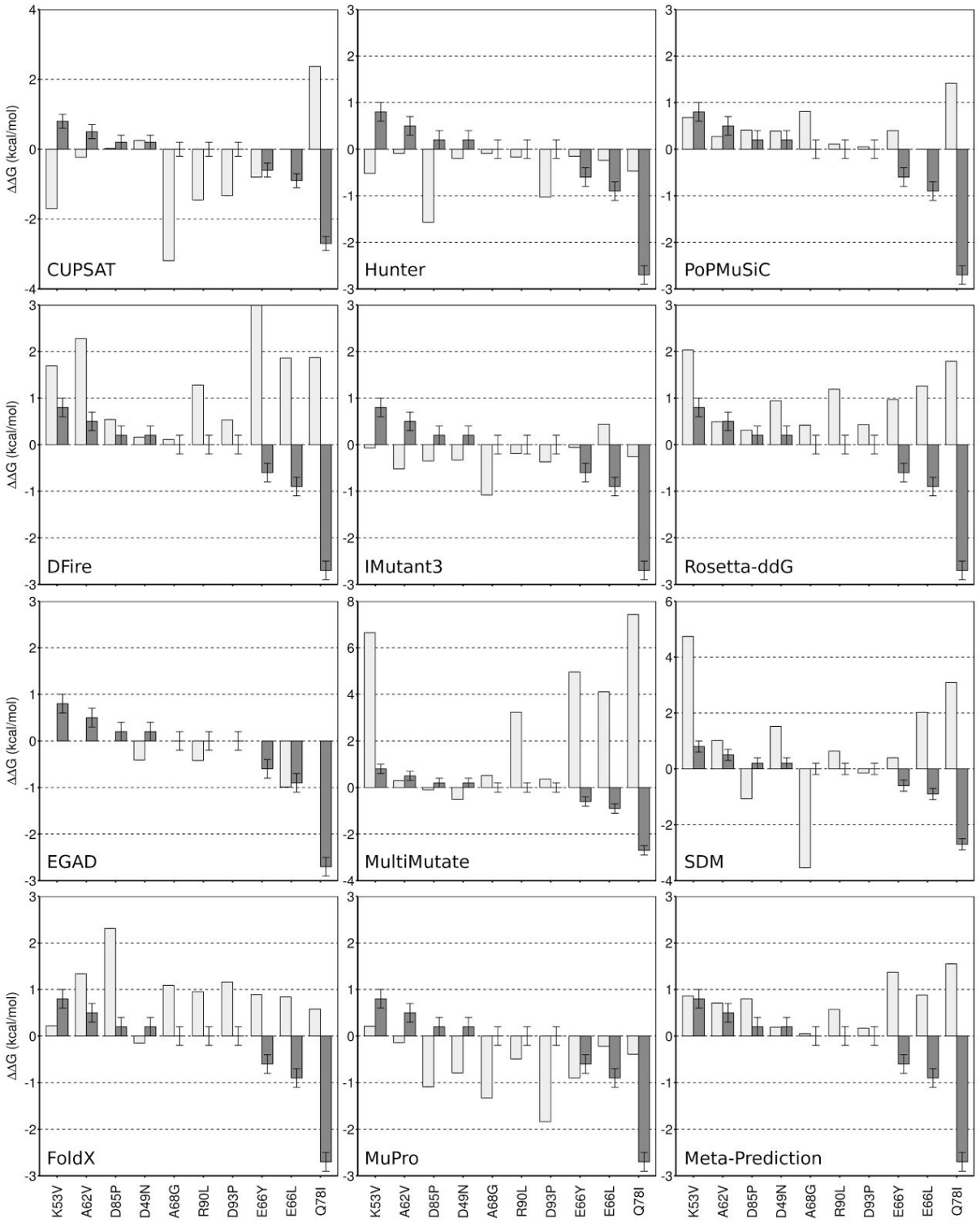

Figure S4: Stability prediction of individual tools on the 10 characterized ThreeFoil mutations. Comparing the predicted with experimentally determined change in stability for the 10 mutations to ThreeFoil shows that none of the individual tools were particularly accurate. Notably, the majority of tools predicted Q78I to be highly stabilizing, and those that did not: Hunter, IMutant3, and MuPro, were generally pessimistic, missing the truly stabilizing mutations. Note that EGAD does not give predictions for mutations to or from glycine and proline, or when more than 2 clashes in VDW volumes are detected (2), thus there are only 3 predictions given here for EGAD.

Table S2: Estimating outcomes of random mutagenesis

Publication	Stabilizing (%)	Destabilizing (%)	Protein Used	Protein Size (structure class)
Araya et al. (3)[1]	2.3	ND	WW domain	34 amino acids (beta)
Foit et al. (4)[2]	1.9	ND	Im7	87 amino acids (alpha)
Deng et al. (5)[3]	2.2	94.9	TEM β-lactamase	263 amino acids (mixed)
Klesmith et al. (6)[4]	3.6	82.1	Levoglucosan kinase	447 amino acids (mixed)
Average	2.5	88.5		

The average % stabilizing across the four publications reporting this value is 2.5%. For the two publications reporting % destabilizing the average is 88.5%, leaving 9.0% as approximately neutral.

Note that the first two publications only determine the number of stabilizing mutations, and do not discriminate between destabilizing and neutral.

[1]of the 646 possible mutations to the 34-residue protein, 15 were found to be stabilizing.

[2]of the 1653 possible mutations to the 87-residue protein, 31 were found to be stabilizing.

[3]a cutoff of > 0.2 $\Delta\Delta G^{stat}$ from the publication was used to count a mutation as stabilizing and < -0.2 for destabilizing in order to match our experimental cutoff of 0.2 kcal/mol. Otherwise the mutation is considered neutral. Note that in this study the screen being used gives a combined measure of stability, solubility, and function.

[4]a cutoff of > 0.15 for the score reported in this publication was used to count a mutation as stabilizing and < -0.15 as destabilizing, as recommended by the authors. In this study the screen being used gives a combined measure of solubility and stability.

Table S3: Tool performance against mutations used in training

Tool	MCC	R	Precision	Accuracy	Standard Error (kcal/mol)
EGAD	0.30	0.53	28%	78%	1.66
FoldX	0.33	0.57	41%	85%	1.67
Rosetta-ddG	0.29	0.53	28%	82%	2.45
CUPSAT	0.32	0.50	41%	86%	1.67
DFire	0.32	0.49	30%	79%	1.95
Hunter	0.25	0.43	30%	82%	2.05
MultiMutate	0.17	0.41	20%	63%	2.54
SDM	0.25	0.42	24%	70%	2.06
PoPMuSiC	0.27	0.60	44%	90%	**1.45**
IMutant3	0.15	0.51	29%	88%	1.57
MuPro[a]	0.40	0.57	**85%**	**92%**	1.46
Meta-Predictor	**0.48**	**0.63**	47%	88%	**1.45**

The best score for each metric is highlighted in bold.

For MCC, Precision and Accuracy, mutations predicted or experimentally determined to have an effect less than 0.2 kcal/mol were not included, thus eliminating a significant source of noise due to the uncertainty in small ΔΔG values.

Values for each metric were determined by randomly sampling 50% of the dataset, computing the metric, repeating this process 1000 times, and reporting the average.

[a]This dataset of 1058 mutations contains mutations used in some of the tool's training sets. Notably for instance, MuPro's training set contained 296 of the mutations tested here. Thus, the anomalously large improvement in MuPro's performance (especially MCC and precision) compared with testing against our primary dataset containing no mutations used for tool training (Table 1), may result from overfitting to the training data.

Table S4: Meta-predictor weight coefficients

Tool	Category	Mutation Type	Weight Coefficient
EGAD	Polarity	Less	0.29
		Same	0.13
		More	0.21
	Size	Smaller	0.18
		Same	0.29
		Larger	0.32
	SASA	Buried	0.36
		Partially Exposed	0.18
		Exposed	0.32
	Secondary Structure	Helical	0.27
		Strand	0.50
		Turn	0.27
		Unstructured	0.26
	Glycine/non-Glycine	Glycine	0.00
		Non-Glycine	0.34
FoldX	Polarity	Less	0.41
		Same	0.23
		More	0.16
	Size	Smaller	0.32
		Same	0.24
		Larger	0.36
	SASA	Buried	0.46
		Partially Exposed	0.22
		Exposed	0.40
	Secondary Structure	Helical	0.44
		Strand	0.31
		Turn	0.36
		Unstructured	0.38

	Glycine/non-Glycine	Glycine	0.27
		Non-Glycine	0.37
Rosetta-ddG	Polarity	Less	0.26
		Same	0.19
		More	0.18
	Size	Smaller	0.26
		Same	0.16
		Larger	0.33
	SASA	Buried	0.45
		Partially Exposed	0.19
		Exposed	0.26
	Secondary Structure	Helical	0.36
		Strand	0.44
		Turn	0.18
		Unstructured	0.10
	Glycine/non-Glycine	Glycine	0.23
		Non-Glycine	0.30
CUPSAT	Polarity	Less	0.12
		Same	0.25
		More	0.29
	Size	Smaller	0.31
		Same	0.04
		Larger	0.15
	SASA	Buried	0.28
		Partially Exposed	0.32
		Exposed	0.14
	Secondary Structure	Helical	0.13
		Strand	0.29
		Turn	0.39

		Unstructured	0.14
	Glycine/non-Glycine	Glycine	0.11
		Non-Glycine	0.24
DFire	Polarity	Less	0.32
		Same	0.43
		More	0.19
	Size	Smaller	0.36
		Same	0.31
		Larger	0.34
	SASA	Buried	0.61
		Partially Exposed	0.39
		Exposed	0.29
	Secondary Structure	Helical	0.51
		Strand	0.50
		Turn	0.16
		Unstructured	0.41
	Glycine/non-Glycine	Glycine	0.01
		Non-Glycine	0.45
Hunter	Polarity	Less	0.12
		Same	0.02
		More	0.05
	Size	Smaller	0.01
		Same	0.08
		Larger	0.23
	SASA	Buried	0.25
		Partially Exposed	0.04
		Exposed	0.13
	Secondary Structure	Helical	0.19
		Strand	0.16

		Turn	0.20
		Unstructured	0.03
	Glycine/non-Glycine	Glycine	0.13
		Non-Glycine	0.15
MultiMutate	Polarity	Less	0.06
		Same	0.02
		More	0.01
	Size	Smaller	0.17
		Same	0.06
		Larger	0.12
	SASA	Buried	0.40
		Partially Exposed	0.13
		Exposed	0.01
	Secondary Structure	Helical	0.30
		Strand	0.17
		Turn	0.00
		Unstructured	0.17
	Glycine/non-Glycine	Glycine	0.08
		Non-Glycine	0.19
SDM	Polarity	Less	0.09
		Same	0.09
		More	0.08
	Size	Smaller	0.22
		Same	0.08
		Larger	0.16
	SASA	Buried	0.38
		Partially Exposed	0.20
		Exposed	0.10
	Secondary Structure	Helical	0.28

		Strand	0.31
		Turn	0.05
		Unstructured	0.09
	Glycine/non-Glycine	Glycine	0.01
		Non-Glycine	0.21
PoPMuSiC	Polarity	Less	0.28
		Same	0.18
		More	0.40
	Size	Smaller	0.32
		Same	0.08
		Larger	0.37
	SASA	Buried	0.42
		Partially Exposed	0.25
		Exposed	0.29
	Secondary Structure	Helical	0.23
		Strand	0.44
		Turn	0.29
		Unstructured	0.37
	Glycine/non-Glycine	Glycine	0.39
		Non-Glycine	0.31
IMutant3	Polarity	Less	0.06
		Same	0.07
		More	0.03
	Size	Smaller	0.08
		Same	0.10
		Larger	0.08
	SASA	Buried	0.26
		Partially Exposed	0.22
		Exposed	0.02

	Secondary Structure	Helical	0.13
		Strand	0.27
		Turn	0.01
		Unstructured	0.07
	Glycine/non-Glycine	Glycine	0.04
		Non-Glycine	0.13
MuPro	Polarity	Less	0.12
		Same	0.13
		More	0.23
	Size	Smaller	0.21
		Same	0.03
		Larger	0.11
	SASA	Buried	0.26
		Partially Exposed	0.24
		Exposed	0.12
	Secondary Structure	Helical	0.08
		Strand	0.26
		Turn	0.21
		Unstructured	0.18
	Glycine/non-Glycine	Glycine	0.00
		Non-Glycine	0.17

The criteria for determining the mutation type, details of obtaining the weighting coefficients, and equation for the simple linear combination of the predictions from each tool are given in the Experimental Procedures.

Supplemental References

1. Broom, A., Doxey, A. C., Lobsanov, Y. D., Berthin, L. G., Rose, D. R., Howell, P. L., McConkey, B. J., and Meiering, E. M. (2012) Modular evolution and the origins of symmetry: reconstruction of a three-fold symmetric globular protein., *Structure* **20**, 161-171.
2. Pokala, N. and Handel, T.M. (2005) Energy functions for protein design: adjustment with protein-protein complex affinities, models for the unfolded state, and negative design of solubility and specificity., *Journal of molecular biology* **347**, 203-227.
3. Araya, C. L., Fowler, D. M., Chen, W., Muniez, I., Kelly, J. W., and Fields, S. (2012) A fundamental protein property, thermodynamic stability, revealed solely from large-scale measurements of protein function., *Proceedings of the National Academy of Sciences of the United States of America* **109**, 16858-16863.
4. Foit, L., Morgan, G. J., Kern, M. J., Steimer, L. R., von Hacht, A. A., Titchmarsh, J., Warriner, S. L., Radford, S. E., and Bardwell, J. C. A. (2009) Optimizing protein stability in vivo., *Molecular cell* **36**, 861-871.
5. Deng, Z., Huang, W., Bakkalbasi, E., Brown, N. G., Adamski, C. J., Rice, K., Muzny, D., Gibbs, R. A., and Palzkill, T. (2012) Deep sequencing of systematic combinatorial libraries reveals β-lactamase sequence constraints at high resolution., *Journal of molecular biology* **424**, 150-167.
6. Klesmith, J. R., Bacik, J.-P., Wrenbeck, E. E., Michalczyk, R., and Whitehead, T. A. (2017) Trade-offs between enzyme fitness and solubility illuminated by deep mutational scanning., *Proceedings of the National Academy of Sciences of the United States of America* **114**, 2265-2270.